EurJIC European Journal of Inorganic Chemistry

ChemPubSoc Europe

FULL PAPER

DOI:10.1002/ejic.201500536

Synthesis and Characterization of Fluorinated β-Ketoiminate Zinc Precursors and Their Utility in the AP-MOCVD Growth of ZnO:F

Samuel D. Cosham,[a] Gabriele Kociok-Köhn,[b] Andrew L. Johnson,*[a] Jeff A. Hamilton,[a] Michael S. Hill,[a] Kieran C. Molloy,[a] and Rémi Castaing[b]

Keywords: Thin films / Chemical vapor deposition / Doping / Zinc oxide / Fluorine

A novel family of zinc bis(β-ketoiminate) complexes **2b–2h** have been synthesized by reaction of the isolated free ligands **1a–h** with dimethylzinc. The isolated zinc complexes were characterized by elemental analysis, NMR spectroscopy, and in the case of **2b–d** and **2f–h**, the molecular structures of the complexes were determined by single-crystal X-ray diffraction which reveals the compounds to be *pseudo*-octahedral six-coordinate, monomeric homoleptic complexes in the solid state. TG analysis showed complexes **2b–f** all to have residual masses at 400 °C of 10 % or less, well below the value for ZnO and thus indicative of volatility. Of these systems **2b** [Zn{MeC(O)CHC(NCH$_2$CH$_2$OMe)CF$_3$}$_2$] has been investigated for its utility in the AP-MOCVD growth of F-doped ZnO (ZnO:F) in the absence of additional oxidant at 400 °C on glass and silicon substrates.

Introduction

Zinc oxide is a versatile, *n*-type wide band gap (3.37 eV) semiconductor material with a lower electron concentration (10^{18}–10^{19} cm^{-3}), compared to ITO (ca. 10^{21} cm^{-3}). Therefore, ZnO is often doped with elements such as B, Al, Ga, F or Cl, to improve electron concentrations.[1] Of these systems fluorine is the most effective dopant with F-doped ZnO (ZnO:F) and ZnO finding application in a number of devices[2] including blue and ultraviolet light emitters,[3] solar cell devices,[4] wave guides[5] and transistors.[6] The piezoelectric properties which ZnO also exhibits makes it useful in the fabrication of microsensors[7] and nanogenerators.[8]

However, central to all these applications is the ability to deposit ZnO and ZnO:F as a thin film of material. Methods for the deposition of thin films of ZnO include electrodeposition,[9] chemical spray pyrolysis,[10] magnetron sputtering,[11] plasma enhanced chemical vapor deposition (PECVD),[12] atomic layer deposition (ALD)[13] and metal-organic chemical vapor deposition (MOCVD).[7b,14] Of these, atmospheric pressure AP-MOCVD has shown itself to be the most promising deposition methodology, because of its application to large scale, large area deposition of thin films, with high growth rates, good conformal coverage and thickness control, all controllable by varying the CVD process parameters. In contrast, doping ZnO with F is difficult and no effective single source precursors for ZnO:F have been reported to date. ZnO:F fabrication has been attempted using a range of techniques including ALD,[15] CVD,[16] spray pyrolysis,[17] RF-magnetron sputtering,[18] laser deposition[19] and electron beam evaporation.[20]

Precursors for ZnO and ZnO:F have focused on various systems including zinc acetates,[21] zinc alkyls (both methyl and ethyl),[16b,22] zinc alkoxides[23] and zinc β-diketonates.[24] In the past the use of ancillary ligands such as H_2O, pyridine, TMEDA or diglyme have been used in conjunction with metal β-diketonates, in an attempt to control the formation of volatile monomeric complexes suited towards CVD applications.[24a,24i,25] However, these complexes are susceptible to loss of ancillary ligands from the coordination sphere of the metal, resulting in the formation of non-volatile oligomeric complexes. In an attempt to ensure the formation of volatile monomeric zinc complexes, we have employed the strategy of using chelating ketoiminate ligands, which incorporate oxygen containing side arms as additional donor ligands.

Latterly, zinc β-ketoiminates have been applied to the ring opening polymerization of cyclic esters,[26] although a

[a] Department of Chemistry, University of Bath, Claverton Down, Bath BA2 7AY, UK
E-mail: a.l.johnson@bath.ac.uk
http://www.bath.ac.uk/chemistry/contacts/academics/andrew_johnson/
[b] Chemical Characterisation and Analysis Facility, Department of Chemistry, University of Bath, Claverton Down, Bath BA2 7AY, UK

Supporting information for this article is available on the WWW under http://dx.doi.org/10.1002/ejic.201500536.

small number zinc β-ketoiminates[14a,14c,27] and β-iminoesterates[28] have previously been investigated for application in MOCVD, where the focus has been on the development of halogen free precursors for exclusive ZnO production.

We have chosen to investigate the application of trifluoromethyl derivatized β-ketoiminate systems, incorporating ether side arms, in the production of novel ZnO precursors. Herein we describe the synthesis, characterization, thermal behavior and preliminary AP-MOCVD results of a family of zinc bis β-ketoiminate complexes.

Results and Discussion

A range of β-ketoiminate ligands **1(a-h)** have been synthesized by a condensation reaction between a β-diketone, either 2,4-pentanedione (Hacac), 1,1,1-trifluoro-2,4-pentanedione (Htfac), 1,1,1-trifluoro-2,4-hexanedione or 1,1,1-trifluoro-5-methyl-2,4-hexanedione respectively and an appropriately functionalized amine (Scheme 1). The free ligands **1b–h** were isolated as pale yellow oils (**f**, **g**), or either white (**b**, **c**, **h**) or pale yellow solids (**d**, **e**) in variable yield, ranging from 21% (**c**) to 62% (**f**).

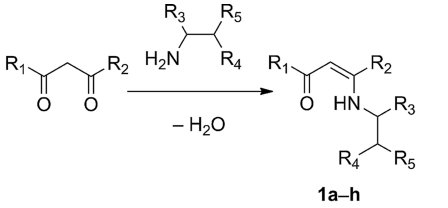

1a–h

	a	b	c	d	e	f	g	h
R_1	Me	CF_3	CF_3	CF_3	CF_3	CF_3	CF_3	CF_3
R_2	Me	Me	Et	^{i}Pr	Me	Me	Me	Me
R_3	H	H	H	H	H	Me	H	H
R_4	H	H	H	H	H	H	OMe	
R_5	OMe	OMe	OMe	OMe	OEt	OMe	OMe	

Scheme 1. General scheme showing the constitution of the ligands **1a–h**.

Zinc complexes of each of these ligands were then prepared by reaction with half a molar equivalent of dimethylzinc (Scheme 2).

Complexes **2a–h** are novel, save for the non-fluorinated complex **2a** which has been previously prepared by others.[14c] Similar non-fluorinated analogues, prepared by others, have incorporated $N(CH_2)_3OMe$,[14c] N*n*Bu, N*n*Pr and N*i*Pr[14a,27a]substituents. Complexes **2b–h** are colourless, air-stable solids and were obtained in good to excellent yields (53–81%). The melting points of these complexes are, somewhat surprisingly, usually higher than the non-fluorinated systems e.g. **2a** (57 °C),[14c] N*n*Bu (72 °C), N*i*Pr (109 °C)[14a] compared to 103–5 °C (**2d**)–141–3 °C (**2b**) for our derivatives, with **2e** (89–91 °C) and **2h** (172–3 °C) being low and high exceptions.

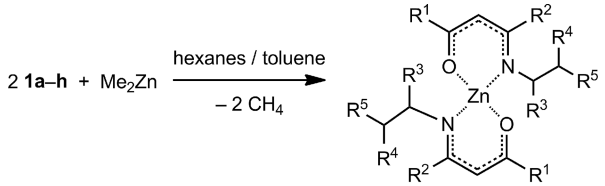

2a–h

Scheme 2. the zinc β-ketoiminate complex **2a–h**.

NMR spectroscopic data for novel **2b–h** show no singlet signals due to {MeZn} moieties confirming the double ligand substitution. Integrals and chemical shifts are consistent with those of the ligands, save for **2f**, where there appears to be four sets of ligand signals in an approximately 1:1:1:5 ratio in the ^{1}H NMR spectrum, resulting from the chiral centre inherent in this ligand which generates a range of diastereomers upon complexation to the zinc. However, despite there being three independent molecules in the asymmetric unit of crystalline **2f** (*see below*), all three are essentially superimposable.

This suggests that while multiple diastereoisomers are present in solution, the system remains fluxional and only one diastereoisomer (an enantiomeric pair as the space group is centrosymmetric) crystallizes out (with minor torsional differences due to packing).

The facile fluxionality of these species suggested by the NMR spectroscopic data for **2f** is supported by NMR spectroscopic data for **2h**, which also incorporates a chiral centre within the ligand. Here, while only one set of ligand resonances are seen within the ^{1}H NMR spectrum at 358 K, cooling generates a more complex spectrum with, for example, four sharp signals (1:1:1:2) in the range δ = 1.30–1.65 ppm due to the methyl group (Scheme 1, R^2 = Me).

All six structures reported (**2b–d**, **2f–g**) show that these species adopt six-coordinate structures with a ZnO_4N_2 coordination sphere, with the ligands acting in a κ^2-*O,N,O* triden-

Table 1. Selected bond lengths [Å] for **2a–d**, **f–h**.

	2a[14c]	**2b**	**2c**[a]			**2d**	**2f**[b]			**2g**	**2h**
			Mol1	Mol2[a]	Mol3[a]		Mol1	Mol2[b]	Mol3[b]		
Zn–O(1)	1.955(1)	2.0167(10)	2.029(2)	2.010(2)	2.007(2)	2.0072(19)	2.0193(17)	2.0291(17)	1.9992(18)	2.0188(17)	2.014(2)
Zn–O(2)	1.939(1)	2.494(2)	2.332(2)	2.385(2)	2.315(3)	2.3466(18)	2.4602(19)	2.5118(18)	2.4382(19)	2.3134(17)	2.360(2)
Zn–O(3)		1.9975(10)	1.999(2)	2.017(2)	2.020(2)	2.0266(19)	2.0227(17)	2.0108(18)	2.0119(17)	2.0161(17)	2.023(2)
Zn–O(4)		2.574(2)	2.415(2)	2.406(2)	2.431(2)	2.4315(18)	2.4078(18)	2.4342(19)	2.5195(19)	2.556(2)	2.365(2)
Zn–N(1)	1.984(2)	2.0368(11)	2.057(2)	2.057(3)	2.071(2)	2.064(2)	2.0404(18)	2.0199(19)	2.0238(19)	2.040(2)	2.056(3)
Zn–N(2)	1.990(2)	2.0313(10)	2.054(2)	2.053(3)	2.063(2)	2.060(2)	2.0471(18)	2.0171(19)	2.0318(19)	2.047(2)	2.049(3)

[a] Zn–O bonds in molecules 2 and 3 refer to O(5)–O(8) and O(9)–O(12), respectively. See Figure S5 for details of the labelling Scheme for molecules 2 and 3. [b] Zn–O bonds in molecules 2 and 3 refer to O(5)–O(8) and O(9)–O(12), respectively. See Figure S6 for details of the labelling Scheme for molecules 2 and 3.

tate chelating mode; the ligands are disposed in a *mer* arrangement with respect to each other (see Figure 1, Table 1, Figures 2, 3, 4, 5, and 6). This is in contrast to complex **2a** which is reported to have a *pseudo* tetrahedral geometry about the zinc centre, such that the oxygen atoms of the pendant ether functionalized side-arms are non-coordinating.[14c] All six species (**2b–d**, **2f–h**) crystallize in centrosymmetric space groups, so chiral **2f** and **2h** crystallize as a single pair of enantiomers. Furthermore, while both **2c** and chiral **2f** crystallize with three molecules in their respective asymmetric units, all three molecules are effectively superimposable i.e. any differences are minor and due to packing effects.

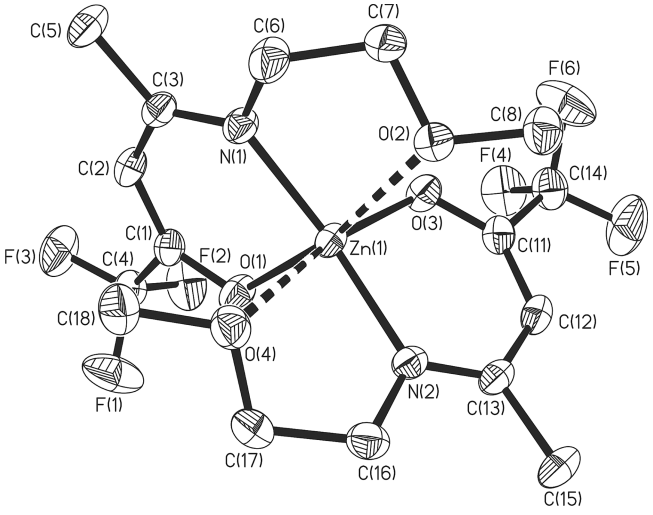

Figure 1. The asymmetric unit of **2b** showing the labelling scheme used in the text and tables thermal ellipsoids are at the 40% level. Key bond lengths are given in Table 1; selected bond angles: O(1)–Zn(1)–O(2) 169.00(4), O(1)–Zn(1)–O(3) 100.05(4), O(1)–Zn(1)–O(4) 88.80(4), O(1)–Zn(1)–N(1) 92.84(4), O(1)–Zn(1)–N(2) 101.19(4), O(2)–Zn(1)–O(3) 84.61(4), O(2)–Zn(1)–O(4) 88.41(4), O(2)–Zn(1)–N(1) 76.24(4), O(2)–Zn(1)–N(2) 88.27(4), O(3)–Zn(1)–O(4) 167.02(4), O(3)–Zn(1)–N(1) 107.97(4), O(3)–Zn(1)–N(2) 94.63(4), O(4)–Zn(1)–N(1) 80.81(4), O(4)–Zn(1)–N(2) 74.18(4), N(1)–Zn(1)–N(2) 150.90(4)°.

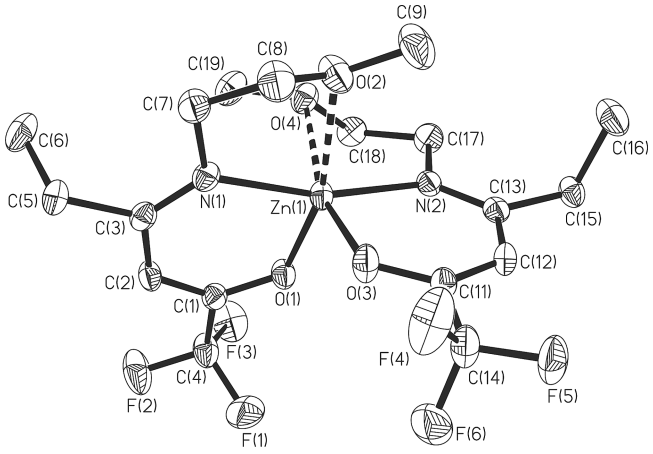

Figure 2. One of three independent molecules in the asymmetric unit of **2c** showing the labelling scheme used in the text and tables thermal ellipsoids are at the 40% level. A view of the complete asymmetric unit is available in the Supplementary Information (Figure S5). Key bond lengths are given in Table 1; selected bond angles: O(1)–Zn(1)–O(2) 162.77(9), O(1)–Zn(1)–O(3) 104.19(10), O(1)–Zn(1)–O(4) 89.75(8), O(1)–Zn(1)–N(1) 92.09(9), O(1)–Zn(1)–N(2) 95.95(9), O(2)–Zn(1)–O(3) 90.36(10), O(2)–Zn(1)–O(4) 77.75(8) N(2), O(2)–Zn(1)–N(1) 76.67(9), O(2)–Zn(1)–N(2) 92.51(9), O(3)–Zn(1)–O(4) 162.94(9), O(3)–Zn(1)–N(1) 97.40(9), O(3)–Zn(1)–N(2) 92.60(9), O(4)–Zn(1)–N(1) 91.76(9). O(4)–Zn(1)–O(2) 75.97(9), N(1)–Zn(1)–N(2) 165.25(10)°.

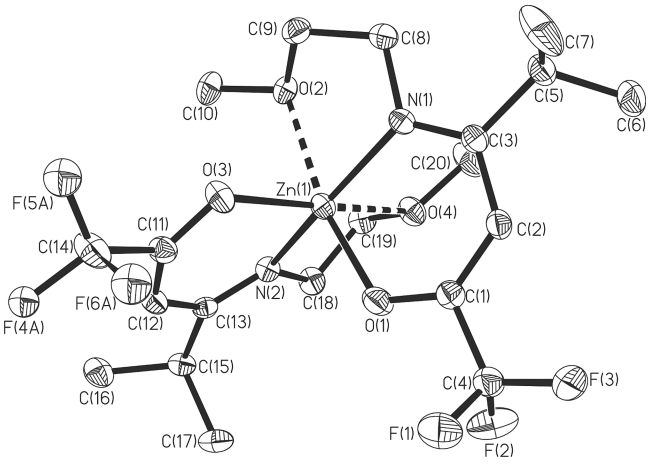

Figure 3. The asymmetric unit of **2d** showing the labelling scheme used in the text and tables thermal ellipsoids are at the 40% level. Key bond lengths are given in Table 1; selected bond angles: O(1)–Zn(1)–O(2) 168.92(7), O(1)–Zn(1)–O(3) 99.32(8), O(1)–Zn(1)–O(4) 91.24(8), O(1)–Zn(1)–N(1) 92.93(8), O(1)–Zn(1)–N(2) 96.67(8), O(2)–Zn(1)–O(3) 87.07(7), O(3)–Zn(1)–O(2) 87.07(7), O(2)–Zn(1)–N(1) 76.69(7), O(2)–Zn(1)–N(2) 92.03(7), O(3)–Zn(1)–O(4) 165.85(7), O(3)–Zn(1)–N(1) 103.81(8), O(3)–Zn(1)–N(2) 92.59(8), O(4)–Zn(1)–N(1) 84.88(7), O(4)–Zn(1)–N(2) 76.75(7), N(1)–Zn(1)–N(2) 159.40(8)°.

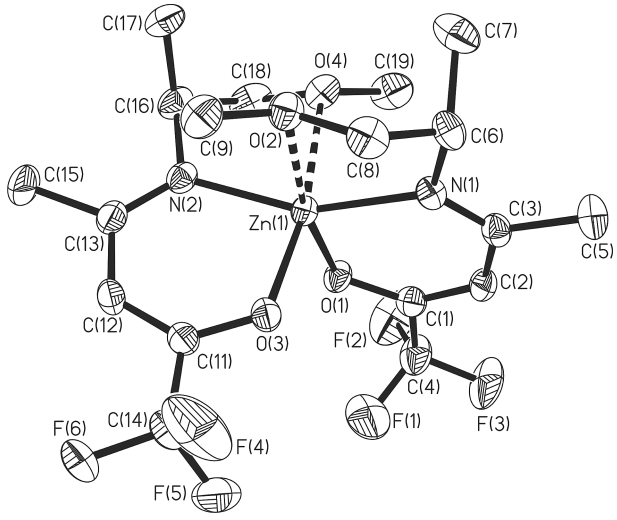

Figure 4. One of three independent molecules in the asymmetric unit of **2f** showing the labelling scheme used in the text and tables thermal ellipsoids are at the 40% level. A view of the complete asymmetric unit is available in the Supporting Information (Figure S6). Key bond lengths are given in Table 1; selected bond angles: O(1)–Zn(1)–O(2) 170.25(6), O(1)–Zn(1)–O(3) 97.68(7), O(1)–Zn(1)–O(4) 85.53(6), O(1)–Zn(1)–N(1) 94.05(6), O(1)–Zn(1)–N(2) 102.27(7), O(2)–Zn(1)–O(3) 87.02(6), O(2)–Zn(1)–O(4) 91.20(6), O(2)–Zn(1)–N(1) 76.65(6), O(2)–Zn(1)–N(2) 85.91(6), O(3)–Zn(1)–O(4) 170.46(6), O(3)–Zn(1)–N(1) 100.53(7), O(3)–Zn(1)–N(2) 93.24(7), O(4)–Zn(1)–N(1) 88.16(7), O(4)–Zn(1)–N(2) 77.27(7), N(1)–Zn(1)–N(2) 157.05(8)°.

Within each ligand, there is one short [1.9975(10)–2.029(2) Å] and one long Zn–O bond [2.3134(17)–2.574(2) Å], the latter resulting from an O:→Zn interaction with the ether lariats, an observation which has been seen previously in related Ba^{II} complexes.[29] These structures are in striking contrast to previously reported **2a**,[14c] which is only four-coordinate at zinc centre as a result of two κ^2-*O*,*N* bidentate ligands. The additional coordination by the ether lariats to the central zinc atom, in the solid-state structures of **2b–d 2f–g**, is presumably in response to the electronic requirements of the Zn^{II} atoms when coordinated to the electron-withdrawing {CF_3} bearing β-ketoiminate ligands. The consequence of this is that both the Zn–O [1.939(1), 1.955(1) Å] and Zn–N bonds [1.984(2), 1.990(2) Å] in **2a** are much shorter (stronger) than those in **2b–d**, **2f–g**; for comparison, Zn–N bonds now reported are in the range 2.1099(19)–2.063(2) Å.

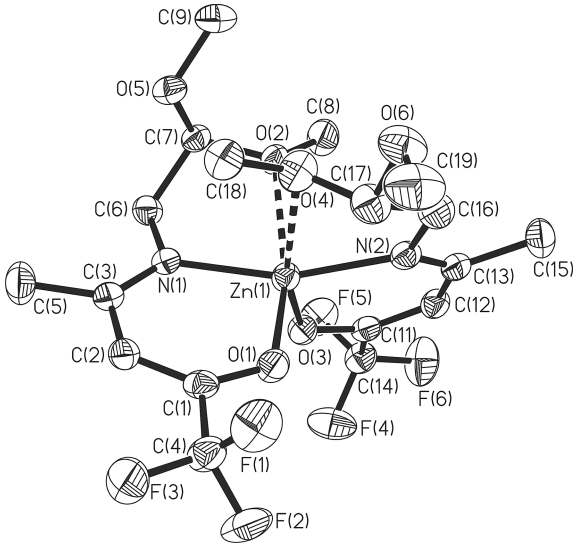

Figure 5. The asymmetric unit of **2g** showing the labelling scheme used in the text and tables thermal ellipsoids are at the 40% level. Key bond lengths are given in Table 1; selected bond angles: O(1)–Zn(1)–O(2) 159.70(7), O(1)–Zn(1)–O(3), 107.69(7), O(1)–Zn(1)–O(4) 86.47(7), O(1)–Zn(1)–N(1) 92.11(8), O(1)–Zn(1)–N(2) 97.18(8), O(2)–Zn(1)–O(3) 90.84(7), O(2)–Zn(1)–O(4) 77.26(7), O(2)–Zn(1)–N(1) 76.65(7), O(2)–Zn(1)–N(2) 89.59(7), O(3)–Zn(1)–O(4) 160.84(7), O(3)–Zn(1)–N(1) 98.49(8), O(3)–Zn(1)–N(2) 93.69(8), O(4)–Zn(1)–N(1) 92.12(8), O(4)–Zn(1)–N(2) 72.82(8), N(1)–Zn(1)–N(2) 161.68(8)°.

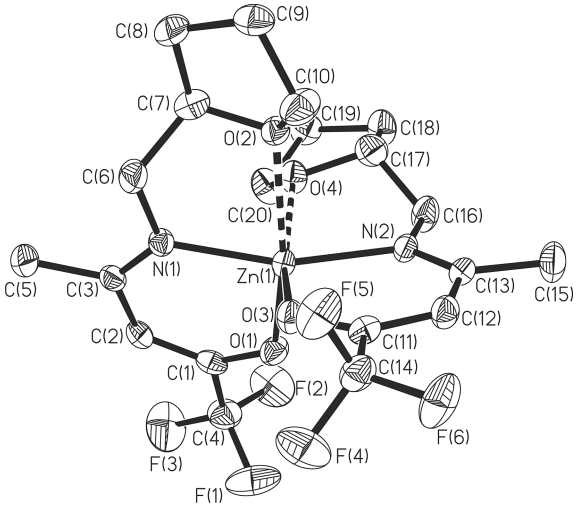

Figure 6. The asymmetric unit of **2h** showing the labelling scheme used in the text and tables thermal ellipsoids are at the 40% level. Key bond lengths are give in Table 1; selected bond angles: O(1)–Zn(1)–O(2) 162.49(10), O(1)–Zn(1)–O(3) 107.32(10), O(1)–Zn(1)–O(4) 88.69(10), O(1)–Zn(1)–N(1) 92.42(11), O(1)–Zn(1)–N(2) 97.28(11), O(2)–Zn(1)–O(3) 88.71(9), O(2)–Zn(1)–O(4) 76.28(9), O(2)–Zn(1)–N(1) 78.26(10), O(2)–Zn(1)–N(2) 88.47(10), O(3)–Zn(1)–O(4) 162.88(10), O(3)–Zn(1)–N(1) 97.37(10), O(3)–Zn(1)–N(2) 93.50(10), O(4)–Zn(1)–N(1) 87.73(10), O(4)–Zn(1)–N(2) 78.11(10), N(1)–Zn(1)–N(2) 162.59(11)°.

Materials Chemistry

TGA data for **2b–h** are shown in Figure 7. Data for **2b–f** all have residual masses at 400 °C of 10% or less, well below the value for ZnO and thus indicative of volatility. These residual masses are slightly higher than seen by others for **2a** (ca. 4% residue),[14c] consistent with their generally higher melting points, but **2b–f** are more thermally stable, showing minimal decomposition/sublimation below 200 °C. The thermal behaviour of precursors, **2g** and **2h**, is strikingly different to other precursors in this series, with residual masses of 24.3 and 23.2% respectively, which are well in excess of the ca. 15% expected for ZnO, presumably due to residual carbon contamination. PXRD analysis of TGA residues from **2b–h** reveal the presence of ZnO.

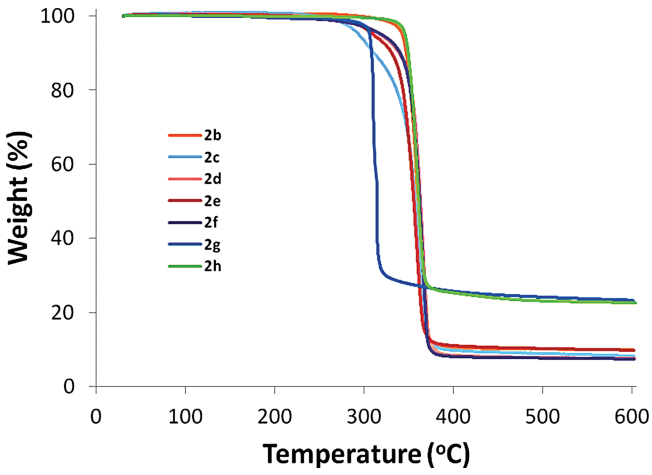

Figure 7. TGA data for complexes **2b–h**.

In an attempt to ascertain possible decomposition pathways for precursor **2b**, TGA-coupled mass spectrometry (TGA-MS) was undertaken. Unfortunately TGA-MS experiments did not yield conclusive results with respect to precursor decomposition pathways, although peaks at *m*/*z* = 58.00 amu and *m*/*z* = 112.01 amu, were observed in the mass spectra. These were attributed to the formation of methyl-vinyl ether and 1,1,1-trifluoropropanone respectively.

As part of our study, vapor pressure measurements were carried out on **2b** using a previously reported method and

apparatus.[30] Details of these analyses for **2b** are depicted in the supporting information. Each set of data was obtained at temperatures below the melting points of the precursors. The vapor pressure of **2b** obeys the general equation $\log P = A - B/T$; where A and B are free parameters, with the corresponding enthalpy of vaporization (ΔH_{vap} = 43.6 ± 0.004 kJ mol^{-1}) being deduced from the parameters, and extrapolates to a pressure of *ca.* 48 Torr at 250 °C. This compares to a calculated value for zinc bis trifluoroacetate, $Zn(tfa)_2$ of 0.83 Torr at 250 °C.[31]

Deposition studies were thus focussed on precursor **2b** as this displayed good volatility (from the TGA data) and was the most cost effect precursor to synthesise (a key precursor requirement) among the group **2b**–**f**. Deposition was carried out at a precursor temperature of 250 °C (due to its thermal stability) and a substrate temperature of 400 °C at atmospheric pressure. No additional reactive gas was added, although a flow of argon gas (5 dm^3/min) was used to assist carryover. Substrates used were microscope slides and silicon ([1,0,0] oriented). Note that in comparison with previous work on film growth from **2a** as a precursor for ZnO, this study is (i) APCVD not LPCVD, (ii) uses the precursor as a single-source with no oxygen source added and (iii) deposits ZnO at a lower onset temperature (400 °C vs. 450–700 °C). While it should be noted that others have reported zinc ketoiminates[27a] and zinc iminoesterate[28] precursors, used to produce ZnO at temperatures as low as 300–350 °C without the need for additional reactive oxidants (i.e. oxygen), it should also be noted that in both cases relatively high carbon contamination throughout the films is reported, and in both cases thermal annealing is required to afford semiconducting materials.

SEM and AFM data for the film grown on glass from **2b** are shown in Figure 8 (a–d). The film is densely packed (Figure 8, a) but at the edges, where the thin films are less densely packed, and pin holes are more obvious, there is evidence of columnar features, made up of hexagonal mesocrystals (Figure 8, b).[32]

This is supported by the PXRD data (Figure 8, e) which shows that the film crystallises in the wurtzite phase and presents a clear [0,0,2] orientation preference i.e. growth along *c*, as seen in the deposition of ZnO from precursor **2a**;[14c] EDX confirms the presence of zinc and oxygen (Supplementary data), with a composition which is slightly oxygen-deficient ($ZnO_{0.89}$).

While EDX measurements failed to detect the presence of fluorine, as indicated by the absence of peaks at 0.68 keV, analysis of the thin films by XPS, reveal F concentrations in the region of 1.1 at.% at the surface. Subsequent etching of the surface for 15 min with an Ar gas cluster ion source at 10 keV beam energy (corresponding to an etching depth of 30 nm) indicates a homogeneous distribution of fluorine throughout the thin films, with F concentrations of 1.2 at.% suggestive of a $ZnO_{(0.9)}$:$F_{(0.02)}$ formulation. Figure 9 shows an XPS spectrum of a ZnO:F thin film after a 15 min etch.

Table 2 shows the calculated atomic percentages of elements from XPS analysis. While XPS analysis shows high carbon contamination levels at the surface, these levels diminish considerably as we move from the surface into the bulk of the materials, down to ca. 2 at.%, a value which is significantly lower than ZnO thin films deposited by related precursors (ca. 10–5.7 %),[27a,28] also produced in the absence of additional oxygen and without the need for annealing in oxygen.

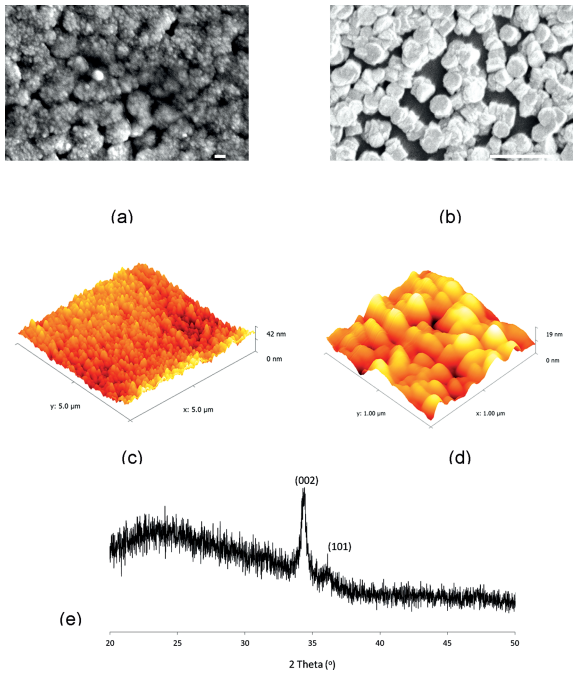

Figure 8. SEM of the film deposited from precursor **2b** at 400 °C on glass, (a) the dense central region, bar length: 1 μm, (b) the film edge, showing columnar hexagonal growth, bar length: 100 nm; AFM of the same film (c) over 5 μm^2, film roughness Rms (Sq) 5.4 nm, Ra (Sa) 4.23 nm, (d) over 1 μm^2, Rms (Sq) 2.9 nm, Ra (Sa) 2.32 nm; (e) PXRD of the film referenced to ZnO (PDF 891397).

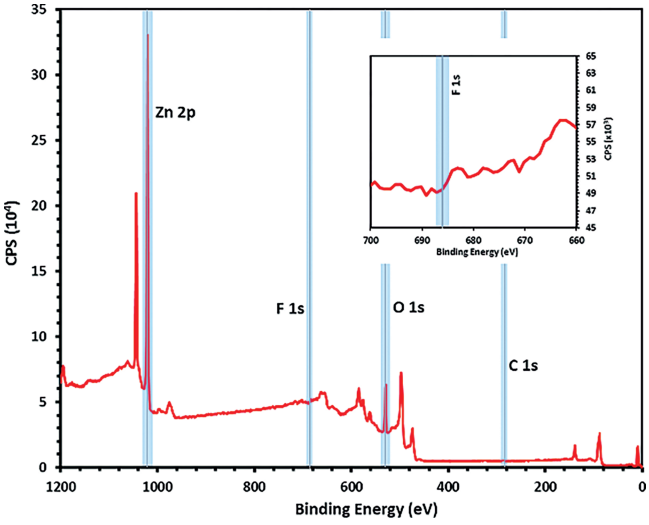

Figure 9. Survey XPS spectrum of a typical film deposited at a substrate temperature of 400 °C and the *1s* regions for fluorine (insert top right).

Table 2. Atomic% of elements in ZnO:F films deposited at 400 °C pre and post-Ar etching (15 min).

Etch time [min]	Atom	% Concentration
0	Zn (2p)	11.13
	O (1s)	35.0
	F (1s)	1.1
	C (1s)	51.8
15	Zn (2p)	51.0
	O (1s)	45.8
	F (1s)	1.2
	C (1s)	2.0

AFM investigation (Figure 8, c, d) showed the films to be relatively smooth, with a root mean square (rms) roughness between approx. 3–5.4 nm over a 1–5 μm^2 range: this compares with rms values of 10 nm for ZnO films prepared by AACVD from toluene solutions of dimethylzinc.[1a] Film thickness was estimated to be 220 nm from the whitish-green color fringe analyzed, and by assuming a refractive index for zinc oxide of 2.0041.[33]

Levels of fluorine incorporation observed in this study are directly comparable to recent reports of ZnO:F thin films produced by ALD,[15] in which fluorine doping concentrations of 1.2% were achieved providing thin films with bulk resistivity values of approx. 1.9×10^{-3} Ωcm. Unfortunately, bulk resistivity values could not be obtained for thin films grown from **2b** at 400 °C, with a deposition time of 30 min, because of incomplete surface coverage. However, thin films (340 nm, estimated as above) grown from **2b** at 400 °C over longer deposition periods (60 min), which apart from being more continuous, have identical analysis features and possess a bulk resistivity of 1.782×10^{-3} Ωcm.

Films were also grown on Si-100 at 400 °C with deposition times of 30 and 60 min respectively, though the results are essentially the same as those described above for deposition on glass; details are given as Supplementary data.

Conclusions

This work documents the synthesis and characterisation of a family of zinc β-ketoiminate complexes with ether functionalised pendent arms, for the growth of ZnO films by MOCVD. The synthesis procedure for both the ligands, and the subsequent zinc complexes, is straight forward and the products can be isolated in good yields and easily scaled up. The molecular structures of six of the complexes **2b**–**d**, **2f**–**h** have been determined revealing the zinc centres to possess six coordinate pseudo octahedral coordination environments. A significant feature of this work is the air and moisture stability of the complexes developed, which are easily handled and are very soluble in a range of common organic solvents, thus negating difficulties with the use of pyrophoric precursors. The thermal properties of complexes **2b**–**f** are encouraging, with moderately low melting points, good volatility and clean decomposition characteristics, which abrogates the use of excessively high temperatures for the deposition of ZnO with carbon incorporation.

Strikingly, complex **2b** appears to be a viable single source precursor for the growth of ZnO:F. The presence of $\{CF_3\}$ groups in the ligand system is in contrast to related precursors, specifically **2a**. Despite attempts to identify a mechanism for fluorine incorporation using TGA-MS analysis we have been unable to elucidate a decomposition pathway, incorporating 1.2% of fluorine within the thin film. **2b** also functions as a single-source with no need for additional oxygen source in the deposition process. While **2b** deposits ZnO:F at a relatively low deposition temperature of 400 °C (vs. 450–700 °C), the thin films produced contain very low levels of carbon contamination in the bulk of the thin film (concentrations at the surface are significantly higher). We feel that these are both significant advances in the development of an atmospheric pressure deposition process compatible with the large scale production of ZnO:F for device fabrication on an industrial/high throughput scale. Our future efforts in reducing the deposition temperature of precursors is ongoing and subsequent research will concentrate in this direction.

Experimental Section

General Information: Manipulations involving organozinc reagents and complexes were performed under an atmosphere of dry argon using standard Schlenk line and glovebox techniques. Hexanes and toluene solvents were dried using a commercially available solvent purification system (Innovative Technology Inc., MA) and degassed under argon prior to use. Deuterated benzene (C_6D_6) NMR solvent was purchased from Fluorochem, UK, and dried with potassium before isolating via vacuum distillation. All dry solvents were stored under argon in Young's ampoules over molecular sieves (4 Å). A toluene solution of dimethylzinc (2 M) was prepared from the neat reagent supplied by SAFC HiTech, UK. All other reagents were purchased from commercial sources and used as supplied.

Melting points were determined utilising a Stuart SMP10 Melting Point Apparatus. Elemental analyses were performed externally by London Metropolitan University Elemental Analysis Service, UK. IR spectra were recorded for the neat sample using a Perkin–Elmer Spectrum 100 FT-IR Spectrometer fitted with a Universal ATR sampling accessory. Spectra were recorded at ambient temperature in the region 4000–650 cm^{-1}. The following abbreviations are used: w (weak), m (medium), s (strong) and br (broad).

Solution ^1H and $^{13}C\{^1H\}$ NMR spectra were recorded with a Bruker Avance 300 spectrometer, whilst ^{19}F NMR spectra were recorded using a Bruker Avance 400 spectrometer. All spectra were obtained at ambient temperature (25 °C). ^1H and ^{13}C NMR chemical shifts are given in ppm and referenced internally to residual non-deuterated solvent resonances. The following abbreviations are used: s (singlet), d (doublet), t (triplet), q (quartet), sept (septet), dd (doublet of doublets), m (multiplet), ap (apparent) and br (broad).

Compounds **1a** and **2a** were synthesized according to literature procedure.[14c]

$F_3CC(O)CHC(CH_3)N(H)CH_2CH_2OCH_3$ (1b): A stirred toluene (300 mL) solution of 1,1,1-trifluoro-2,4-pentanedione (40.0 mL, 331 mmol) was treated with 2-methoxyethylamine (28.8 mL, 331 mmol) and refluxed using a Dean–Stark apparatus for 24 h. The resulting reaction mixture was dried using $MgSO_4$, filtered and volatiles then removed in vacuo to afford an orange-brown oil. The oil

was washed with hot hexanes (2 × 150 mL) and the hexanes layer decanted. The hexanes washings were combined and cooled to 0 °C to afford the product as off-white crystalline needles. The product was subsequently isolated by filtration, washed with cold hexanes and air-dried, yield 39.63 g, 57%, m.p. 57–58 °C. Microanalysis: found (calcd. for $C_8H_{12}F_3NO_2$): C 45.36 (45.50), H 5.81 (5.73), N 6.54 (6.63) %. IR (neat): $\tilde{\nu}$ = 3004.3 (w), 2940.9 (br. w), 2902.4 (br. w), 1677.0 (br. w), 1586.3 (br. s), 1544.7 (m), 1525.7 (m), 1458.7 (m), 1439.1 (w), 1392.4 (w), 1367.5 (w), 1347.5 (w), 1301.8 (m), 1261.4 (w), 1246.6 (br. m), 1195.7 (m), 1168.9 (br. m), 1111.4 (s), 1065.9 (s), 1018.5 (m), 1008.2 (m), 955.7 (w), 871.9 (m), 846.5 (s), 767.2 (s), 754.2 (s), 722.9 (s) cm^{-1}. ^1H NMR (300 MHz, C_6D_6): δ = 11.46–10.97 (br. s, 1 H, NH), 5.25 (s, 1 H, CH), 2.87 (s, 3 H, OCH_3), 2.72 [t, ^3J(H,H) = 5.3 Hz, 2 H, CH_2O], 2.55–2.47 (m, 2 H CH_2N), 1.20 (s, 3 H, CCH_3) ppm. $^{13}C\{^1H\}$ NMR (75.5 MHz, C_6D_6): δ = 175.8 (q, $^2J_{C,F}$ = 32.0 Hz, CO), 169.3 (s, CN), 118.8 (q, $^1J_{C,F}$ = 288.6 Hz, CF_3), 89.5 (s, CH), 70.8 (s, CH_2O), 58.6 (s, OCH_3), 43.3 (s,CH_2N), 18.7 (s, CCH_3) ppm. ^{19}F NMR (376.5 MHz, C_6D_6): δ = –76.1 (s) ppm.

$F_3CC(O)CHC(CH_2CH_3)N(H)CH_2CH_2OCH_3$ (1c): A stirred toluene (100 mL) solution of 1,1,1-trifluoro-2,4-hexanedione (6.72 g, 40 mmol) was treated with 2-methoxyethylamine (3.48 mL, 40 mmol) and refluxed using a Dean–Stark apparatus for 24 h. The resulting reaction mixture was dried using $MgSO_4$, filtered and volatiles then removed in vacuo to afford an orange-brown oil. The oil was washed with hot hexanes (2 × 50 mL) and the hexanes layer decanted. The hexanes washings were combined and cooled to 0 °C to afford the product as off-white crystalline needles. The product was subsequently isolated by filtration, washed with cold hexanes and air-dried, yield 1.88 g, 21%, m.p. 36–37 °C. Microanalysis: found (calcd. for $C_9H_{14}F_3NO_2$): C 47.82 (48.00), H 6.15 (6.27), N 6.08 (6.22) %. IR (neat): $\tilde{\nu}$ = 2973.6 (br. w), 2928.5 (w), 2895.2 (br. w), 2830.3 (w), 1681.9 (br. w), 1594.1 (br. s), 1550.3 (w), 1534.3 (w), 1483.5 (w), 1472.9 (w), 1454.0 (m), 1439.6 (m), 1398.4 (w), 1382.1 (w), 1353.9 (w), 1314.7 (m), 1267.4 (m), 1247.3 (w), 1234.1 (br. m), 1194.0 (w), 1179.1 (s), 1110.7 (s), 1050.1 (m), 1017.5 (m), 949.5 (m), 865.0 (s), 838.7 (m), 793.2 (w), 772.9 (s), 752.5 (s), 723.1 (s), 681.1 (m) cm^{-1}. ^1H NMR (300 MHz, C_6D_6): δ_H = 11.54–11.13 (br. s, 1 H, NH), 5.32 (s, 1 H, CH), 2.96 (s, 3 H, OCH_3), 2.90 (t, $^3J_{H,H}$ = 5.2 Hz, 2 H, CH_2O), 2.74 (ap q, $^3J_{H,H}$ = 5.3 Hz, 2 H, CH_2N), 1.68 (q, $^3J_{H,H}$ = 7.6 Hz, 2 H, CH_2CH_3) 0.66 (t, $^3J_{H,H}$ = 7.6 Hz, 3 H, CH_2CH_3) ppm. $^{13}C\{^1H\}$ NMR (75.5 MHz, C_6D_6): δ_C = 175.8 (q, $^2J_{C,F}$ = 32.0 Hz, CO), 174.4 (s, CN), 118.8 (q, $^1J_{C,F}$ = 288.9 Hz, CF_3), 87.2 (q, $^3J^{C,F}$ = 1.5 Hz, CF_3), 70.7 (s, CH_2O), 58.6 (s, OCH_3), 43.0 (s,CH_2N), 25.2 (s, CH_2CH_3), 11.4 (s, CH_2CH_3) ppm. ^{19}F NMR (376.5 MHz, C_6D_6): δ_F = –76.1 (s) ppm.

$F_3CC(O)CHC[CH(CH_3)_2]N(H)CH_2CH_2OCH_3$ (1d): A stirred toluene (100 mL) solution of 1,1,1-trifluoro-5-methyl-2,4-hexanedione (2.98 mL, 20 mmol) was treated with 2-methoxyethylamine (1.74 mL, 20 mmol) and refluxed using a Dean–Stark apparatus for 24 h. The resulting reaction mixture was dried using $MgSO_4$, filtered and volatiles then removed in vacuo to afford an orange-brown oil. Distillation of the crude oil under reduced pressure affords the pure product as very pale yellow crystals upon cooling, yield 2.71 g, 57%, m.p. 28–29 °C. Microanalysis: found (calcd. for $C_{10}H_{16}F_3NO_2$): C 50.43 (50.20), H 6.79 (6.74), N 6.01 (5.85) %. IR (neat): $\tilde{\nu}$ = 2980.7 (w), 2933.7 (w), 2897.5 (br. w), 2837.5 (w), 1604.6 (w), 1576.9 (s), 1465.7 (w), 1452.9 (br. m), 1403.3 (w), 1387.3 (m), 1369.1 (w), 1339.8 (w), 1282.6 (w), 1246.1 (s), 1237.0 (s), 1176.7 (br. s), 1118.8 (s), 1109.4 (s), 1081.2 (w), 1054.6 (w), 1021.1 (s), 968.8 (w), 930.8 (w), 897.7 (w), 873.8 (s), 842.6 (br. m), 773.9 (s), 742.2 (s), 715.4 (s), 692.8 (s) cm^{-1}. ^1H NMR (300 MHz, C_6D_6): δ_H = 11.82–11.46 (br. s, 1 H, NH), 5.45 (s, 1 H, CH), 2.98 (s, 3 H, OCH_3), 2.94 (t, ^3JH,H = 5.2 Hz, 2 H, CH_2O), 2.87–2.80 (m, 2 H CH_2N), 2.27 (sept, ^3JH,H = 6.8 Hz, 1 H, $CHCH_3$), 0.74 (s, ^3JH,H = 6.8 Hz, 6 H, $CHCH_3$) ppm. $^{13}C\{^1H\}$ NMR (75.5 MHz, C_6D_6): δ_C = 178.9 (s, CN), 176.0 (q, $^2J_{C,F}$ = 31.8 Hz, CO), 118.9 (q, $^1J_{C,F}$ = 288.6 Hz, CF_3), 84.0 (q, $^3J_{C,F}$ = 1.6 Hz, CH), 70.7 (s, CH_2O), 58.7 (s, OCH_3), 42.6 (s,CH_2N), 28.9 (s, $CHCH_3$), 20.4 (s, $CHCH_3$) ppm. ^{19}F NMR (376.5 MHz, C_6D_6): δ_F = –76.1 (s) ppm.

$F_3CC(O)CHC(CH_3)N(H)CH_2CH_2OCH_2CH_3$ (1e): A stirred toluene (100 mL) solution of 1,1,1-trifluoro-2,4-pentanedione (2.43 mL, 20 mmol) was treated with 2-ethoxyethylamine (2.10 mL, 20 mmol) and refluxed using a Dean–Stark apparatus for 4 h. The resulting reaction mixture was dried using $MgSO_4$, filtered and volatiles then removed in vacuo to afford a golden oil. The crude oil was washed with hot hexanes (2 × 25 mL) and the hexanes layer decanted. The hexanes washings were combined and cooled to –28 °C to afford the product as a pale yellow solid. The product was subsequently isolated by filtration, washed with cold hexanes and air-dried, yield 1.76 g, 39%, m.p. 27–29 °C. Microanalysis: found (calcd. for $C_9H_{14}F_3NO_2$): C 48.29 (48.00), H 6.15 (6.27), N 6.41 (6.22) %. IR (neat): $\tilde{\nu}$ = 2980.1 (m), 2936.3 (w), 2890.3 (w), 2855.6 (m), 2798.7 (w), 1587.9 (br. s), 1548.5 (m), 1529.1 (m), 1457.0 (m), 1445.9 (br. m), 1410.0 (m), 1374.4 (m), 1347.1 (w), 1304.3 (m), 1249.4 (br. s), 1171.0 (br. m), 1114.6 (br. s), 1071.1 (m), 1045.1 (m), 1012.1 (w), 960.2 (m), 930.0 (m), 871.7 (s), 840.7 (s), 768.8 (s), 755.6 (s), 723.7 (s) cm^{-1}. ^1H NMR (300 MHz, C_6D_6): δ = 11.51–11.02 (br. s, 1 H, NH), 5.25 (s, 1 H, CH), 3.07 (q, $^3J_{H,H}$ = 7.0 Hz, 2 H, CH_2CH_3), 2.85 (t, $^3J_{H,H}$ = 5.2 Hz, 2 H, CH_2CH_2O), 2.58 (ap q, $^3J_{H,H}$ = 5.5 Hz, 2 H CH_2N), 1.24 (s, 3 H, CH_3CN), 0.99 (t, $^3J_{H,H}$ = 7.0 Hz, 3 H, CH_3CH_2) ppm. $^{13}C\{^1H\}$ NMR (75.5 MHz, C_6D_6): δ = 175.7 (q, ^2JC,F = 31.8 Hz, CO), 169.3 (s, CN), 118.8 (q, $^1J_{C,F}$ = 289.4 Hz, CF_3), 89.4 (q, $^3J_{C,F}$ = 1.5 Hz, CH), 68.7 (s, CH_2CH_2O), 66.7 (s, CH_2CH_3), 43.5 (s,CH_2N), 18.7 (s, CH_3CN), 15.1 (s, CH_3CH_2) ppm. ^{19}F NMR (376.5 MHz, C_6D_6): δ = –76.1 (s) ppm.

$F_3CC(O)CHC(CH_3)N(H)CH(CH_3)CH_2OCH_3$ (1f): A stirred toluene (100 mL) solution of 1,1,1-trifluoro-2,4-pentanedione (3.64 mL, 30 mmol) was treated with 1-methoxy-2-propylamine (3.16 mL, 30 mmol) and refluxed using a Dean–Stark apparatus for 2 h. The resulting reaction mixture was dried using $MgSO_4$, filtered and volatiles then removed in vacuo to afford a golden oil. Distillation of the crude oil under reduced pressure affords the pure product as a yellow oil, yield 4.16 g, 62%. Microanalysis: found (calcd. for $C_9H_{14}F_3NO_2$): C 47.87 (48.00), H 6.31 (6.27), N 6.36 (6.22) %. IR (neat): $\tilde{\nu}$ = 2984.3 (br. w), 2936.7 (br. w), 2884.0 (br. w), 2836.6 (br. w), 1679.7 (br. w), 1615.8 (w), 1579.2 (s), 1446.8 (br. m), 1391.1 (w), 1372.7 (m), 1244.8 (s), 1182.1 (m), 1105.1 (br. s), 1029.2 (w), 992.0 (w), 961.6 (m), 926.6 (w), 907.5 (br. w), 866.3 (m), 813.5 (br. m), 800.3 (w), 769.0 (m), 740.6 (m), 725.9 (s) cm^{-1}. ^1H NMR (300 MHz, C_6D_6): δ = 11.60–11.07 (br. s, 1 H, NH), 5.25 (s, 1 H, CHCO), 3.24–3.08 (m, 1 H, $CHCH_3$), 2.91 (s, 3 H, CH_3O), 2.78–2.65 (m, 2 H CH_2), 1.40 (s, 3 H, CH_3CN), 0.71 (d, $^3J_{H,H}$ = 6.6 Hz, 3 H, CH_3CH) ppm. $^{13}C\{^1H\}$ NMR (75.5 MHz, C_6D_6): δ = 175.7 (q, $^2J_{C,F}$ = 32.1 Hz, CO), 168.8 (s, CN), 118.8 (q, $^1J_{C,F}$ = 289.6 Hz, CF_3), 89.4 (q, $^3J_{C,F}$ = 1.5 Hz, CHCO), 76.2 (s, CH_2), 58.8 (s, CH_3O), 49.7 (s, $CHCH_3$), 18.8 (s, CH_3CN), 17.6 (s, CH_3CH) ppm. ^{19}F NMR (376.5 MHz, C_6D_6): δ = –76.2 (s) ppm.

$F_3CC(O)CHC(CH_3)N(H)CH_2CH(OCH_3)_2$ (1g): A stirred toluene (100 mL) solution of 1,1,1-trifluoro-2,4-pentanedione (2.43 mL, 20 mmol) was treated with aminoacetaldehyde dimethylacetal (2.18 mL, 20 mmol) and refluxed using a Dean–Stark apparatus for 4 h. The resulting reaction mixture was dried using $MgSO_4$, filtered and volatiles then removed in vacuo to afford a golden oil. Distillation of the crude oil under reduced pressure affords the pure prod-

uct as a yellow oil, yield 1.96 g, 41%. Microanalysis: found (calcd. for $C_9H_{14}F_3NO_3$): C 44.92 (44.81), H 5.70 (5.85), N 5.77 (5.81) %. IR (neat): $\tilde{\nu}$ = 3006.7 (br. w), 2943.1 (br. w), 2838.9 (w), 1725.5 (br. w), 1619.3 (m), 1579.0 (br. s), 1442.5 (br. m), 1393.4 (w), 1370.7 (m), 1295.1 (w), 1242.2 (br. s), 1183.1 (s), 1120.8 (s), 1104.4 (s), 1076.1 (br. s), 979.3 (m), 925.5 (w), 890.7 (m), 869.1 (w), 823.0 (br. m), 770.5 (m), 741.2 (s), 725.9.9 (s) cm^{-1}. ^1H NMR (300 MHz, C_6D_6): δ = 11.34–11.00 (br. s, 1 H, NH), 5.25 (s, 1 H, CHCO), 3.89 (t, $^3J_{H,H}$ = 5.4 Hz, 1 H, CHO), 3.01 (s, 6 H, OCH_3), 2.82 (ap t, $^3J_{H,H}$ = 5.7 Hz, 2 H, CH_2N), 1.29 (s, 3 H, CCH_3) ppm. $^{13}C\{^1H\}$ NMR (75.5 MHz, C_6D_6): δ = 175.8 (q, $^2J_{C,F}$ = 32.3 Hz, CO), 169.6 (s, CN), 118.6 (q, $^1J_{C,F}$ = 289.0 Hz, CF_3), 102.8 (s, CHO), 89.7 (q, $^3J_{C,F}$ = 1.5 Hz, CHCO), 54.5 (s, OCH_3), 45.6 (s,CH_2N), 18.8 (s, CCH_3) ppm. ^{19}F NMR (376.5 MHz, C_6D_6): δ = –76.2 (s) ppm.

$F_3CC(O)CHC(CH_3)N(H)CH_2(CHOCH_2CH_2CH_2)$ (1h): A stirred toluene (100 mL) solution of 1,1,1-trifluoro-2,4-pentanedione (2.43 mL, 20 mmol) was treated with tetrahydrofurfurylamine (2.06 mL, 20 mmol) and refluxed using a Dean–Stark apparatus for 4 h. The resulting reaction mixture was dried using $MgSO_4$, filtered and volatiles then removed in vacuo to afford a golden oil. The crude oil was washed with hot hexanes (2 × 10 mL) and the hexanes layer decanted. The hexanes washings were combined and cooled to ambient temperature resulting in crystallisation of the product as an off-white crystalline solid. The product was subsequently isolated by filtration, washed with cold hexanes and air-dried, yield 1.25 g, 26%, m.p. 66–68 °C. Microanalysis: found (calcd. for $C_{10}H_{14}F_3NO_2$): C 50.50 (50.63), H 5.84 (5.95), N 5.88 (5.90) %. IR (neat): $\tilde{\nu}$ = 2986.3 (w), 2977.4 (w), 2863.2 (br. w), 1676.5 (br. w), 1590.2 (br. s), 1540.9 (m), 1520.8 (w), 1491.5 (w), 1457.8 (m), 1391.1 (w), 1370.1 (br. w), 1294.9 (m), 1251.1 (br. s), 1167.0 (m), 1132.4 (w), 1117.8 (s), 1063.9 (s), 993.6 (w), 953.7 (w), 923.8 (w), 887.2 (m), 836.5 (s), 809.1 (w), 763.3 (s), 747.7 (s), 723.0 (s) cm^{-1}. ^1H NMR (300 MHz, C_6D_6): δ = 11.54–11.11 (br. s, 1 H, NH), 5.27 (s, 1 H, CHCO), 3.62–3.40 (s, 1 H, CH_2O), 3.45–3.29 (m, 2 H, CHO, CH_2O), 2.69–2.55 (m, 1 H, CH_2N), 2.53–2.38 (m, 1 H, CH_2N), 1.45–1.19 (m, 6 H, CH_2CHO, CH_2CH_2O, CH_3), 1.10–0.91 (m, 1 H, CH_2CHO) ppm. $^{13}C\{^1H\}$ NMR (75.5 MHz, C_6D_6): δ = 175.8 (q, $^2J_{C,F}$ = 32.2 Hz, CO), 169.6 (s, CN), 118.8 (q, $^1J_{C,F}$ = 288.6 Hz, CF_3), 89.6 (q, $^3J_{C,F}$ = 1.5 Hz, CHCO), 77.1 (s, CHO), 68.4 (s, CH_2O), 46.9 (s, CH_2N), 28.5 (s, CH_2CHO), 25.9 (s, CH_2CH_2O), 18.8 (s, CH_3) ppm. ^{19}F NMR (376.5 MHz, C_6D_6): δ = –76.1 (s) ppm.

$Zn[F_3CC(O)CHC(CH_3)NCH_2CH_2OCH_3]_2$ (2b): A stirred solution of **1b** (4.22 g, 20 mmol) in 50 mL hexanes was slowly treated with a 2 M toluene solution of dimethylzinc (5.0 mL, 10 mmol), affording a white precipitate. After stirring for 24 h volatiles were removed in vacuo and the resultant residue recrystallized from toluene at 4 °C to afford the product as colourless crystals, yield 3.34 g, 69%, m.p. 141–143 °C. Microanalysis: found (calcd. for $C_{16}H_{22}F_6N_2O_4Zn$): C 39.51 (39.56), H 4.62 (4.57), N 5.73 (5.77) %. IR (neat): $\tilde{\nu}$ = 2915.0 (br. w), 2843.3 (br. w), 1614.8 (s), 1534.7 (s), 1482. 2 (m), 1451.3 (m), 1377.3 (w), 1356.1 (w), 1282.6 (s), 1248.1 (w), 1170.5 (m), 1148.4 (m), 1116.6 (s), 1081.2 (s), 1032.7 (m), 1011.0 (w), 973.7 (w), 880.2 (s), 863.6 (m), 825.8 (w), 773.9 (s), 743.0 (w), 727.5 (s), 629.9 (w) cm^{-1}. ^1H NMR (300 MHz, C_6D_6): δ = 5.26 (s, 1 H, CH), 3.61–3.18 (br. s, 1 H, OCH_2), 3.16–2.89 (br. s, 3 H, OCH_2, NCH_2), 2.88 (s, 3 H, OCH_3), 1.30 (s, 3 H, CCH_3) ppm. $^{13}C\{^1H\}$ NMR (75.5 MHz, C_6D_6): δ = 174.3 (s, CN), 164.7 (q, $^2J_{C,F}$ = 30.7 Hz, CO), 120.8 (q, $^1J_{C,F}$ = 284.3 Hz, CF_3), 93.6 (q, $^3J_{C,F}$ = 2.8 Hz, CH), 70.1 (s, CH_2O), 58.2 (s, OCH_3), 50.0 (s, CH_2N), 22.2 (s, CCH_3) ppm. ^{19}F NMR (376.5 MHz, C_6D_6): δ = –74.3 (s) ppm.

$Zn[F_3CC(O)CHC(CH_2CH_3)NCH_2CH_2OCH_3]_2$ (2c): A stirred solution of **1c** (0.45 g, 2 mmol) in 20 mL hexanes was slowly treated with a 2 M toluene solution of dimethylzinc (0.5 mL, 1 mmol), affording a white precipitate. After stirring for 48 h volatiles were removed in vacuo and the resultant residue recrystallized from toluene at 4 °C to afford the product as colourless crystals, yield 0.41 g, 80%, m.p. 119–120 °C. Microanalysis: found (calcd. for $C_{18}H_{26}F_6N_2O_4Zn$): C 41.96 (42.08), H 5.06 (5.10), N 5.34 (5.45) %. IR (neat): $\tilde{\nu}$ = 2966.3 (w), 2926.5 (br. w), 2879.4 (w), 2840.9 (br. w), 1610.0 (s), 1534.4 (s), 1484.8 (br. m), 1376.9 (w), 1364.4 (w), 1321.5 (w), 1286.1 (s), 1268.2 (w), 1221.2 (w), 1171.3 (m), 1148.6 (m), 1110.1 (s), 1082.3 (m), 1042.7 (w), 1023.9 (m), 881.9 (s), 849.4 (w), 810.0 (br. m), 773.4 (s), 741.1 (w), 726.9 (s), 692.0 (w) cm^{-1}. ^1H NMR (300 MHz, C_6D_6): δ = 5.30 (s, 1 H, CH), 3.47–3.23 (br. s, 1 H, OCH_2), 3.11–2.94 (br. s, 3 H, OCH_2, NCH_2), 2.92 (s, 3 H, OCH_3), 1.74–1.55 (br. s, 2 H, CH_2CH_3), 0.64 (t, $^3J_{H,H}$ = 7.7 Hz, 3 H, CH_2CH_3) ppm. $^{13}C\{^1H\}$ NMR (75.5 MHz, C_6D_6): δ = 178.8 (s, CN), 165.4 (q, $^2J_{C,F}$ = 30.8 Hz, CO), 120.8 (q, $^1J_{C,F}$ = 284.0 Hz, CF_3), 91.8 (q, $^3J_{C,F}$ = 2.8 Hz, CH), 70.5 (s, CH_2O), 58.4 (s, OCH_3), 49.1 (s, CH_2N), 28.4 (s, CH_2CH_3), 11.5 (s, CH_2CH_3) ppm. ^{19}F NMR (376.5 MHz, C_6D_6): δ = –74.3 (s) ppm.

$Zn[F_3CC(O)CHC(CH\{CH_3\}_2)NCH_2CH_2OCH_3]_2$ (2d): A stirred solution of **1d** (0.48 g, 2 mmol) in 20 mL hexanes was slowly treated with a 2 M toluene solution of dimethylzinc (0.5 mL, 1 mmol), affording a white precipitate. After stirring for 48 h volatiles were removed in vacuo and the resultant residue recrystallized from toluene at 4 °C to afford the product as colourless crystals, yield 0.44 g, 81%, m.p. 103–105 °C. Microanalysis: found (calcd. for $C_{20}H_{30}F_6N_2O_4Zn$): C 44.30 (44.33), H 5.41 (5.58), N 5.10 (5.17) %. IR (neat): $\tilde{\nu}$ = 2968.1 (br. m), 2935.8 (br. w), 2846.6 (br. w), 1609.1 (s), 1560.3 (w), 1526.5 (s), 1496.9 (m), 1463.5 (m), 1431.4 (w), 1391.8 (w), 1368.3 (w), 1338.9 (w), 1284.5 (s), 1242.7 (w), 1173.5 (m), 1153.0 (s), 1124.2 (s), 1107.9 (br. s), 1074.4 (m), 1037.1 (m), 1019.4 (m), 924.7 (w), 879.3 (s), 839.2 (w), 800.8 (w), 776.5 (s), 741.6 (w), 717.8 (s), 703.6 (w) cm^{-1}. ^1H NMR (300 MHz, C_6D_6): δ = 5.48 (s, 1 H, CHCO), 3.53–3.24 (br. s, 1 H, OCH_2), 3.22–3.04 (br. s, 3 H, OCH_2, NCH_2), 2.95 (s, 3 H, OCH_3), 2.50 (sept, $^3J_{H,H}$ = 6.8 Hz, 1 H, $CHCH_3$), 0.72 (d, $^3J_{H,H}$ = 6.8 Hz, 6 H, $CHCH_3$) ppm. $^{13}C\{^1H\}$ NMR (75.5 MHz, C_6D_6): δ = 182.6 (s, CN), 165.6 (q, $^2J_{C,F}$ = 30.6 Hz, CO), 120.9 (q, $^1J_{C,F}$ = 283.5 Hz, CF_3), 87.3 (q, $^3J_{C,F}$ = 2.9 Hz, CHCO), 70.6 (s, CH_2O), 58.4 (s, OCH_3), 48.6 (s, CH_2N), 30.4 (s, $CHCH_3$) 20.3 (s, $CHCH_3$) ppm. ^{19}F NMR (376.5 MHz, C_6D_6): δ = –74.3 (s) ppm.

$Zn[F_3CC(O)CHC(CH_3)NCH_2CH_2OCH_2CH_3]_2$ (2e): A stirred solution of **1e** (0.45 g, 2 mmol) in 20 mL hexanes was slowly treated with a 2 M toluene solution of dimethylzinc (0.5 mL, 1 mmol), affording a white precipitate. After stirring for 48 h volatiles were removed in vacuo and the resultant residue recrystallized from toluene at 4 °C to afford the product as colourless crystals, yield 0.34 g, 66%, m.p. 89–91 °C. Microanalysis: found (calcd. for $C_{18}H_{26}F_6N_2O_4Zn$): C 41.87 (42.08), H 5.00 (5.10), N 5.57 (5.45) %. IR (neat): $\tilde{\nu}$ = 2978.3 (br. w), 2878.3 (br. w), 1614.5 (s), 1530.8 (s), 1483.4 (m), 1377.7 (m), 1351.4 (w), 1286.0 (s), 1149.6 (m), 1112.5 (br. s), 1070.0 (w), 1036.9 (w), 927.1 (m), 875.8 (s), 790.7 (m), 774.6 (s), 727.9 (s) cm^{-1}. ^1H NMR (300 MHz, C_6D_6): δ = 5.28 (s, 1 H, CH), 3.41–3.12 (m, 4 H, CH_3CH_2, CH_2CH_2N), 3.01 (t, $^3J_{H,H}$ = 5.4 Hz, 2 H, CH_2N), 1.32 (s, 3 H, CH_3CN), 0.90 (t, $^3J_{H,H}$ = 7.1 Hz, 3 H, CH_3CH_2) ppm. $^{13}C\{^1H\}$ NMR (75.5 MHz, C_6D_6): δ = 175.3 (s, CN), 164.6 (q, $^2J_{C,F}$ = 31.3 Hz, CO), 120.6 (q, $^1J_{C,F}$ = 284.0 Hz, CF_3), 94.1 (q, $^3J_{C,F}$ = 2.9 Hz, CH), 68.3 (s, CH_2CH_2N), 66.4 (s, CH_3CH_2), 51.0 (s, CH_2N), 22.2 (s, CH_3CN), 14.7 (s, CH_3CH_2) ppm. ^{19}F NMR (376.5 MHz, C_6D_6): δ = –74.3 (s) ppm.

$Zn[F_3CC(O)CHC(CH_3)NCH(CH_3)CH_2OCH_3]_2$ (2f): A stirred solution of **1f** (0.45 g, 2 mmol) in 15 mL hexanes was slowly treated with

a 2 M toluene solution of dimethylzinc (0.5 mL, 1 mmol), resulting in the slow formation of a white precipitate. After stirring for 24 h volatiles were removed in vacuo and the resultant residue recrystallized from toluene at –28 °C to afford the product as colourless crystals, yield 0.27 g, 53%, m.p. 134–136 °C. Microanalysis: found (calcd. for $C_{18}H_{26}F_6N_2O_4Zn$): C 41.96 (42.08), H 4.97 (5.10), N 5.50 (5.45) %. IR (neat): $\tilde{\nu}$ = 2935.6 (br. w), 2905.5 (br. w), 2841.1 (br. w), 1606.7 (s), 1526.3 (s), 1484.3 (m), 1470.6 (m), 1449.0 (w), 1387.0 (br. w), 1280.6 (s), 1165.8 (m), 1136.5 (m), 1116.8 (s), 1091.4 (s), 1069.6 (s), 923.7 (s), 900.0 (m), 862.6 (s), 840.4 (w), 789.9 (w), 768.7 (w), 759.8 (s), 727.0 (s), 663.1 (w) cm^{-1}. ^1H NMR (300 MHz, C_6D_6): δ = 5.28 (s, 1 H, CHCO), 5.26 (s, 2 H, CHCO), 5.20 (s, 5 H, CHCO), 3.53 (dd, $^2J_{H,H}$ = 8.7, $^3J_{H,H}$ = 3.4 Hz, 5 H, CH_2), 3.50–3.34 (m, 3 H, $CHCH_3$), 3.30–3.21 (m, 5 H, $CHCH_3$), 3.12–3.06 (m, 2 H, CH_2), 3.05 (s, 3 H, CH_3O), 3.01–2.94 (m, 4 H, CH_2), 2.93 (s, 15 H, CH_3O), 2.90 (s, 3 H, CH_3O), 2.87 (dd, $^2J_{H,H}$ = 8.7, $^3J_{H,H}$ = 2.6 Hz, 5 H, CH_2), 2.84 (s, 3 H, CH_3O), 1.54 (s, 3 H, CH_3CN), 1.41 (s, 3 H, CH_3CN), 1.39 (s, 3 H, CH_3CN), 1.37 (s, 15 H, CH_3CN), 1.08 (d, $^3J_{H,H}$ = 6.6 Hz, 3 H, CH_3CH), 0.99–96 (m, 6 H, CH_3CH), 0.94 (d, $^3J_{H,H}$ = 6.6 Hz, 15 H, CH_3CH) ppm. $^{13}C\{^1H\}$ NMR (75.5 MHz, C_6D_6): δ = 174.4 (s, CN), 173.8 (s, CN), 173.3 (s, CN), 172.8 (s, CN), 165.1–163.5 (m, CO), 120.7 (q, $^1J_{C,F}$ = 284.1 Hz, CF_3), 94.6 (q, $^3J_{C,F}$ = 2.9 Hz, CHCO), 94.2–94.0 (m, CHCO), 93.5 (q, $^3J_{C,F}$ = 2.9 Hz, CHCO), 76.3 (s, CH_2), 76.0 (s, CH_2), 75.9 (s, CH_2), 74.8 (s, CH_2), 58.9 (s, CH_3O), 58.7 (s, CH_3O), 58.5 (s, CH_3O), 58.4 (s, CH_3O), 55.7 (s, $CHCH_3$), 55.5 (s, $CHCH_3$), 55.4 (s, $CHCH_3$), 54.8 (s, $CHCH_3$), 22.4 (s, CH_3CN), 22.1 (s, CH_3CN), 21.7 (s, CH_3CN), 21.5 (s, CH_3CN), 18.1 (s, CH_3CH), 18.1 (s, CH_3CH), 18.0 (s, CH_3CH), 17.9 (s, CH_3CH) ppm. ^{19}F NMR (376.5 MHz, C_6D_6): δ = –74.4 (s), –74.4 (s), –74.5 (s), –74.5 (s) ppm.

$Zn[F_3CC(O)CHC(CH_3)NCH_2CH(OCH_3)_2]_2$ (2g): A stirred solution of **1g** (0.48 g, 2 mmol) in 20 mL toluene was slowly treated with a 2 M toluene solution of dimethylzinc (0.5 mL, 1 mmol). After stirring for 24 h volatiles were removed in vacuo and the resultant residue recrystallized from toluene at 4 °C to afford the product as colourless crystals, yield 0.36 g, 66%, m.p. 131–132 °C. Microanalysis: found (calcd. for $C_{18}H_{26}F_6N_2O_6Zn$): C 39.49 (39.61), H 4.88 (4.80), N 5.07 (5.13) %. IR (neat): $\tilde{\nu}$ = 2944.0 (br. w), 2835.7 (br. w), 1617.7 (s), 1533.3 (s), 1480.2 (m), 1442.9 (w), 1372.0 (w), 1282.6 (s), 1169.5 (m), 1150.1 (m), 1116.6 (s), 1093.8 (m), 1082.7 (m), 1064.6 (m), 1037.0 (w), 981.9 (m), 907.5 (m), 878.8 (s), 778.3 (s), 729.1 (s), 702.6 (w) cm^{-1}. ^1H NMR (300 MHz, C_6D_6): δ = 5.28 (s, 1 H, CHCO), 4.43 (t, $^3J_{H,H}$ = 5.4 Hz, 1 H, $CHCH_2$), 3.29–3.08 (br. s, 2 H, CH_2), 3.04 (s, 6 H, OCH_3), 1.29 (s, 3 H, CCH_3) ppm. $^{13}C\{^1H\}$ NMR (75.5 MHz, C_6D_6): δ = 175.3 (s, CN), 164.9 (q, $^2J_{C,F}$ = 30.8 Hz, CO), 120.7 (q, $^1J_{C,F}$ = 283.8 Hz, CF_3), 103.0 (s, $CHCH_2$), 94.1 (q, $^3J_{C,F}$ = 2.9 Hz, CHCO), 55.0–53.1 (br. s, OCH_3), 52.7 (s, CH_2), 22.4 (s, CCH_3) ppm. ^{19}F NMR (376.5 MHz, C_6D_6): δ = –74.4 (s) ppm.

$Zn[F_3CC(O)CHC(CH_3)NCH_2(CHOCH_2CH_2CH_2)]_2$ (2h): A stirred solution of **1h** (0.47 g, 2 mmol) in 20 mL toluene was slowly treated with a 2 M toluene solution of dimethylzinc (0.5 mL, 1 mmol). After stirring for 24 h volatiles were removed in vacuo and the resultant residue recrystallized from toluene at 4 °C to afford the product as colourless crystals, yield 0.39 g, 73%, m.p. 172–173 °C. Microanalysis: found (calcd. for $C_{20}H_{26}F_6N_2O_4Zn$): C 44.57 (44.67), H 4.74 (4.87), N 5.24 (5.21) %. IR (neat): $\tilde{\nu}$ = 2984.1 (br. w), 2878.0 (br. w), 1618.6 (s), 1536.2 (s), 1480.6 (m), 1428.4 (w), 1369.2 (w), 1284.4 (s), 1170.1 (m), 1148.0 (m), 1114.3 (s), 1067.1 (m), 1018.5 (m), 973.5 (w), 924.7 (w), 897.2 (s), 873.2 (w), 843.2 (w), 821.9 (w), 777.3 (s), 744.0 (w), 727.2 (s), 681.5 (br. w) cm^{-1}. ^1H NMR (300 MHz, C_6D_6): δ = 5.30 (s, 1 H, CHCO), 4.18–3.26 (br. m, 3 H, CHO, CH_2O), 3.17–2.66 (br. s, 2 H, CH_2N), 1.64–1.30 (br. m, 6 H, CH_2CHO, CH_2CH_2O, CH_3), 1.14–0.86 (br. s, 1 H, CH_2CHO) ppm. $^{13}C\{^1H\}$ NMR (75.5 MHz, C_6D_6): δ = 172.1 (s, CN), 164.6 (q, $^2J_{C,F}$ = 30.4 Hz, CO), 121.0 (q, $^1J_{C,F}$ = 284.4 Hz, CF_3), 93.3 (s, CH), 78.0–77.0 (br. s, CHO), 67.5 (s, CH_2O), 54.6–54.0 (br. s, CH_2N), 29.1–28.7 (m, CH_2CHO), 25.5–25.2 (m, CH_2CH_2O), 22.1 (s, CH_3) ppm. ^{19}F NMR (376.5 MHz, C_6D_6): δ = –74.2 (s) ppm.

Crystallography: Experimental details relating to the single-crystal X-ray crystallographic study is summarised in Table 3. Data for **2b** and **2g** were collected on a Nonius Kappa CCD diffractometer at 150(2) K using Mo-K_α radiation (λ = 0.71073 Å). Data for **2c**, **2d**, **2f** and **2h** were collected on a SuperNova X-ray diffraction systems at 150(2) K using Cu-K_α radiation (λ = 1.54184 Å). All structures were solved by direct methods and refined on F^2 data using the

Table 3. Crystal data for **2b**–**2d**, **2f**–**2h**.

	2b	**2c**	**2d**	**2f**	**2g**	**2h**
formula	$C_{16}H_{22}F_6N_2O_4Zn$	$C_{54}H_{78}F_{18}N_6O_{12}Zn_3$	$C_{20}H_{30}F_6N_2O_4Zn$	$C_{54}H_{78}F_{18}N_6O_{12}Zn_3$	$C_{18}H_{26}F_6N_2O_6Zn$	$C_{20}H_{26}F_6N_2O_4Zn$
Formula mass	485.72	1541.33	541.83	1541.33	545.78	537.80
Crystal system	triclinic	monoclinic	orthorhombic	triclinic	monoclinic	monoclinic
Space group	$P\bar{1}$	$P2_1/c$	$Pbca$	$P\bar{1}$	$P21/a$	$P2_1/n$
a [Å]	8.7940(2)	13.9631(5)	16.1188(2)	10.219(5)	8.7920(2)	8.8344(3)
b [Å]	10.5640(2)	34.8902(12)	14.4041(2)	17.605(5)	25.2010(7)	19.4647(7)
c [Å]	12.2410(2)	13.6491(4)	20.7733(2)	19.921(5)	10.7110(3)	13.2940(5)
α [°]	103.4670(10)	90	90	70.345(5)	90	90
β [°]	102.2550(10)	91.427(3)	90	82.648(5)	106.954(2)	100.619(4)
γ [°]	109.1090(10)	90	90	86.481(5)	90	90
Unit cell volume [$Å^3$]	992.14(3)	6647.4(4)	4823.08(10)	3347(2)	2270.06(11)	2246.87(14)
Temperature [K]	150(2)	150(2)	150(2)	150(2)	150(2)	150(2)
Z	2	4	8	2	4	4
Radiation type	Mo-K_α	Mo-K_α	Cu-K_α	Mo-K_α	Mo-K_α	Cu-K_α
Absorption coefficient, μ [mm^{-1}]	1.318	1.184	2.100	1.176	1.168	2.253
Reflections measured	18043	25905	32288	35335	20213	7825
Independent reflections	5288	14795	4535	18211	5050	4146
R_{int}	0.0344	0.0326	0.0559	0.0306	0.0652	0.0401
Final R_1 values [$I>2\sigma(I)$]	0.0285	0.0525	0.0504	0.0422	0.0423	0.0601
Final $wR(F^2)$ values [$I>2\sigma(I)$]	0.0765	0.0978	0.1295	0.0825	0.1022	0.1669
Final R_1 values (all data)	0.0332	0.0730	0.0519	0.0762	0.0632	0.0638
Final $wR(F^2)$ values (all data)	0.0802	0.1059	0.1312	0.0944	0.1126	0.1706
Goodness of fit	1.018	1.077	1.026	1.006	1.049	1.071

WinGX-1.70 suite of programmes.[34] All hydrogen atoms are included in idealised positions and refined using the riding model.

The asymmetric unit of **2c** and **2f** both consist of three independent, but essentially similar, molecules. One of the three molecules in the asymmetric unit cell of **2c** [centred around Zn(2)] possesses disorder in one of the ethyl groups attached to a β-ketoiminate ligand; the disorder has been modelled isotropically over two positions using a free variable. Complex **2d** has disorder in the three fluorine atoms attached to C(14), the disorder has been modelled isotropically over two positions using a free variable to calculate occupancy factors.

CCDC-1400741 (for **2b**), -1400742 (for **2c**), -1400743 (for **2d**), -1400744 (for **2f**), -1400745 (for **2g**), -1400746 (for **2h**) contain the supplementary crystallographic data for this paper. These data can be obtained free of charge from The Cambridge Crystallographic Data Centre via www.ccdc.cam.ac.uk/data_request/cif.

Materials Chemistry: Thermogravimetric analyses (TGA) were obtained using a Perkin–Elmer TGA4000 thermogravimetric analyzer. Analyses were performed air-sensitively, with the samples sealed under an atmosphere of argon in crimped aluminium TGA pans. Data points were collected every second at a ramp rate of 10 °C min^{-1} in a flowing (20 mL min^{-1}) N_2 stream. Vapor pressure data for complex **2b** was obtained externally at SAFC HiTech, Bromborough, UK.

TGA-MS data was obtained using a Setsys Evolution TGA 16/18 by Setaram, equipped with a S-type thermocouple and an alumina crucible of 170 µL. Analysis was performed under an argon flow (20 mL/min) at a heating rate of 5 K/min. Evolving gas is taken off from the TG analysis chamber to the Mass Spec through a stainless steel capillary The associated mass spectrometer is an Omnistar GSD 320 (Pfeiffer Vacuum), equipped with a quadrupole mass analyser (1–200 amu and mass scan rate of 200 ms/amu) and a Faraday detector.

SEM images were taken using a JEOL FESEM 6301F, while AFM analysis was carried out on a Nanosurf Flexafm easyscan 2 instrument with a Tap 190 AL/G AFM tip and 10 nm tip radius (Tapping mode). Film analysis by PXRD was made using a Bruker D8 Advance diffractometer.

X-ray photoelectron spectrsocopy (XPS) measurements were performed by the Matrerials & Surface Science Institute (Service) at the University of Limerick, Eire, on a Kratos Axis Ultra photoelectron spectrometer, utilising monochromatic Al-K_a radiation (photon energy 1486.6 eV). The instrument was pre-calabrated using the C 1s line at 284.8 eV. Samples were sputtered for a pre-determined set time over a 4 mm wide area using 4 kV argon ions using a minibeam I ion source. Spectra were collected at pass energies of 160 eV, with the 100 mm apperature in place to focus on the centre of the etch pit.

Sheet resistivity measurements were recorded using a Jandel Multiheight 4-point probe in combination with a Guardian Surface Resistivity Meter Model #SRM-232–100, with a sheet resistance range of 0–100 ohm/sq.

Deposition of ZnO was carried out using a home-built reactor similar to that reported by others.[35] In a typical experiment, dry argon carrier gas was passed at a rate of approximately 5 dm^3/min through a mineral oil bubbler (3–4 bubbles/sec) and into a quartz tube (o.d. 21 mm, i.d. 19 mm, length 220 mm) via a glass delivery tube fitted into a drilled natural rubber bung. The quartz tube was housed in a Carbolite MTF 10/25/130 tube furnace set to maintain a temperature of 250 °C with the open end allowed to rest onto an Infrared Salamander (HTE 500 W/230 V) ceramic heater. The substrate was then introduced into the open end of the quartz tube and the ceramic heater set to maintain a temperature of 400 °C. The apparatus was allowed to equilibrate under a flow of argon gas. A small quartz sample boat was loaded evenly with approximately 0.10 g of the precursor under study. The carrier gas flow was halted temporarily in order to allow the positioning of the sample boat in the region of the quartz tube encompassed within the tube furnace. The carrier gas flow was re-initiated and the deposition commenced simultaneously upon the melting of the precursor within the quartz boat. Deposition was carried out for 30 min.

Acknowledgments

The authors thank Engineering and Physical Sciences Research Council (EPSRC) for funding (grant numbers EP/F056494/1 and EP/1019278/1)

[1] a) D. S. Bhachu, G. Sankar, I. P. Parkin, *Chem. Mater.* **2012**, *24*, 4704–4710; b) Y. Liu, Y. Li, H. Zeng, *J. Nanomater.* **2013**, 1–9.
[2] a) H. Morkoç, Ü. Özgür, *Zinc oxide: Fundamentals, Materials and Device Technology*, Wiley-VCH, Weinheim, Germany, **2009**; b) R. Kumar, G. Kumar, O. Al-Dossary, A. Umar, *Mater. Express* **2015**, *5*, 3–23.
[3] S. Tüzemen, E. Gür, *Opt. Mater.* **2007**, *30*, 292–310.
[4] a) C. Battaglia, J. Escarre, K. Soderstrom, M. Charriere, M. Despeisse, F. J. Haug, C. Ballif, *Nat. Photonics* **2011**, *5*, 535–538; b) L. Li, T. Zhai, Y. Bando, D. Golberg, *Nano Energy* **2012**, *1*, 91–106.
[5] E. J. Ibanga, C. Le Luyer, J. Mugnier, *Mater. Chem. Phys.* **2003**, *80*, 490–495.
[6] A. M. Ma, M. Gupta, F. R. Chowdhury, M. Shen, K. Bothe, K. Shankar, Y. Tsui, D. W. Barlage, *Solid-State Electron.* **2012**, *76*, 104–108.
[7] a) M. Z. Yang, C. L. Dai, C. C. Wu, *Sensors* **2011**, *11*, 11112–11121; b) S. Pati, P. Banerji, S. B. Majumder, *Sens. Actuators A* **2014**, *213*, 52–58; c) X. Pan, X. Zhao, *Sensors* **2015**, *15*, 8919–8930.
[8] a) Z. L. Wang, J. H. Song, *Science* **2006**, *312*, 242–246; b) E. Lee, J. Park, M. Yim, Y. Kim, G. Yoon, *Appl. Phys. Lett.* **2015**, *106*.
[9] B. N. Illy, A. C. Cruickshank, S. Schumann, R. Da Campo, T. S. Jones, S. Heutz, M. A. McLachlan, D. W. McComb, D. J. Riley, M. P. Ryan, *J. Mater. Chem.* **2011**, *21*, 12949.
[10] J. De Merchant, M. Cocivera, *Chem. Mater.* **1995**, *7*, 1742–1749.
[11] a) K. Ellmer, *J. Phys. D* **2000**, *33*, R17–R32; b) L. Liang, Z. Huang, L. Cai, W. Chen, B. Wang, K. Chen, H. Bai, Q. Tian, B. Fan, *ACS Appl. Mater. Interfaces* **2014**, *6*, 20585–20589.
[12] a) M. D. Barankin, E. Gonzalez Ii, A. M. Ladwig, R. F. Hicks, *Sol. Energy Mater. Sol. Cells* **2007**, *91*, 924–930; b) D. Bekermann, A. Gasparotto, D. Barreca, L. Bovo, A. Devi, R. A. Fischer, O. I. Lebedev, C. Maccato, E. Tondello, G. Van Tendeloo, *Cryst. Growth Des.* **2010**, *10*, 2011–2018; c) D. Bekermann, A. Gasparotto, D. Barreca, A. Devi, R. A. Fischer, M. Kete, U. L. Stangar, O. I. Lebedev, C. Maccato, E. Tondello, G. Van Tendeloo, *ChemPhysChem* **2010**, *11*, 2337–2340; d) K. W. Johnson, S. Guruvenket, R. A. Sailer, S. P. Ahrenkiel, D. L. Schulz, *Thin Solid Films* **2013**, *548*, 210–219.
[13] a) A. Illiberi, F. Roozeboom, P. Poodt, *ACS Appl. Mater. Interfaces* **2012**, *4*, 268–272; b) T. Tynell, M. Karppinen, *Semicond. Sci. Technol.* **2014**, *29*, 043001.
[14] a) J. S. Matthews, O. O. Onakoya, T. S. Ouattara, R. J. Butcher, *Dalton Trans.* **2006**, 3806–3811; b) D. Bekermann, D. Pilard, R. A. Fischer, A. Devi, *ESC Trans.* **2009**, *25*, 601–608; c) D. Bekermann, D. Rogalla, H. W. Becker, M. Winter, R. A. Fischer, A. Devi, *Eur. J. Inorg. Chem.* **2010**, 1366–1372; d) D. Bekermann, A. Ludwig, T. Toader, C. Maccato, D. Barreca, A. Gasparotto, C. Bock, A. D. Wieck, U. Kunze, E. Tondello, R. A. Fischer, A. Devi, *Chem. Vapor Depos.* **2011**, *17*, 155–161; e) J.

Holmes, K. Johnson, B. Zhang, H. E. Katz, J. S. Matthews, *Appl. Organomet. Chem.* **2012**, *26*, 267–272.

[15] Y. J. Choi, H. H. Park, *J. Mater. Chem. A* **2014**, *2*, 98–108.

[16] a) J. H. Hu, R. G. Gordon, *Sol. Cells* **1991**, *30*, 437–450; b) A. L. Johnson, A. J. Kingsley, G. Kociok-Köhn, K. C. Molloy, A. L. Sudlow, *Inorg. Chem.* **2013**, *52*, 5515–5526.

[17] a) A. Guillen-Santiago, M. D. L. Olvera, A. Maldonado, A. Reyes, R. Asomoza, *Phys. Status Solidi A* **2002**, *191*, 499–508; b) A. D. Olvera, A. Maldonado, R. Asomoza, S. Tirado-Guerra, *Thin Solid Films* **2002**, *411*, 198–202.

[18] F. H. Wang, C. F. Yang, Y. H. Lee, *Nanoscale Res. Lett.* **2014**, *9*, 97.

[19] Y. Thimont, J. Clatot, M. Nistor, C. Labrugère, A. Rougier, *Sol. Energy Mater. Sol. Cells* **2012**, *107*, 136–141.

[20] H. Y. Xu, Y. C. Liu, R. Mu, C. L. Shao, Y. M. Lu, D. Z. Shen, X. W. Fan, *Appl. Phys. Lett.* **2005**, *86*, 123107.

[21] a) A. K. Gyani, O. F. Z. Khan, P. O'Brien, D. S. Urch, *Thin Solid Films* **1989**, *182*, L1–L4; b) O. F. Z. Khan, P. O'Brien, *Thin Solid Films* **1989**, *173*, 95–97; c) J. S. Kim, H. A. Marzouk, P. J. Reucroft, C. E. Hamrin Jr., *Thin Solid Films* **1992**, *217*, 133–137; d) T. Maruyama, J. Shionoya, *J. Mater. Sci. Lett.* **1992**, *11*, 170–172; e) K. Kobayashi, T. Matsubara, S. Matsushima, S. Shirakata, S. Isomura, G. Okada, *Thin Solid Films* **1995**, *266*, 106–109; f) S. Jain, T. T. Kodas, M. Hampden-Smith, *Chem. Vapor Depos.* **1998**, *4*, 51–59.

[22] a) S. Suh, D. M. Hoffman, L. M. Atagi, D. C. Smith, *J. Mater. Sci. Lett.* **1999**, *18*, 789–791; b) B. S. Li, Y. C. Liu, Z. Z. Zhi, D. Z. Shen, Y. M. Lu, J. Y. Zhang, X. W. Fan, *J. Cryst. Growth* **2002**, *240*, 479–483; c) A. Velasco, T. Oguchi, H.-J. Kim, *J. Cryst. Growth* **2009**, *311*, 2731–2735; d) S. Ashraf, A. C. Jones, J. Bacsa, A. Steiner, P. R. Chalker, P. Beahan, S. Hindley, R. Odedra, P. A. Williams, P. N. Heys, *Chem. Vapor Depos.* **2011**, *17*, 45–53; e) R. Kanjolia, A. C. Jones, S. Ashraf, J. Bacsa, K. Black, P. R. Chalker, P. Beahan, S. Hindley, R. Odedra, P. A. Williams, P. N. Heys, *J. Cryst. Growth* **2011**, *315*, 292–296; f) S. Hindley, A. C. Jones, S. Ashraf, J. Bacsa, A. Steiner, P. R. Chalker, P. Beahan, P. A. Williams, R. Odedra, *J. Nanosci. Nanotechnol.* **2011**, *11*, 8294–8301.

[23] a) A. L. Johnson, N. Hollingsworth, G. Kociok-Köhn, K. C. Molloy, *Inorg. Chem.* **2008**, *47*, 12040–12048; b) V. Sallet, C. Thiandoume, J. F. Rommeluere, A. Lusson, A. Riviere, J. P. Riviere, O. Gorochov, R. Triboulet, V. Munoz-Sanjose, *Mater. Lett.* **2002**, *53*, 126–131.

[24] a) A. Gulino, F. Castelli, P. Dapporto, P. Rossi, I. Fragala, *Chem. Mater.* **2000**, *12*, 548–554; b) Y. Kashiwaba, K. Sugawara, K. Haga, H. Watanabe, B. P. Zhang, Y. Segawa, *Thin Solid Films* **2002**, *411*, 87–90; c) M. Losurdo, M. M. Giangregorio, P. Capezzuto, G. Bruno, G. Malandrino, M. Blandino, I. L. Fragala, *Mater. Res. Soc. Symp. Proc.* **2006**, *891*, 387–392; d) M. Losurdo, M. M. Giangregorio, A. Sacchetti, P. Capezzuto, G. Bruno, G. Malandrino, I. L. Fragala, *J. Mater. Res.* **2006**, *21*, 1632–1637; e) L. V. Saraf, M. H. Engelhard, C. M. Wang, A. S. Lea, D. E. McCready, V. Shutthanandan, D. R. Baer, S. A. Chambers, *J. Mater. Res.* **2007**, *22*, 1230–1234; f) C. Pflitsch, A. Nebatti, G. Brors, B. Atakan, *J. Cryst. Growth* **2012**, *348*, 5–9; g) C. H. Lee, D. W. Kim, *J. Electroceram.* **2014**, *33*, 12–16; h) S. Kuprenaite, T. Murauskas, A. Abrutis, V. Kubilius, Z. Saltyte, V. Plausinaitiene, *Surf. Coat. Technol.* **2015**, *271*, 156–164; i) G. Malandrino, M. Blandino, L. M. S. Perdicaro, I. L. Fragala, P. Rossi, P. Dapporto, *Inorg. Chem.* **2005**, *44*, 9684–9689.

[25] a) G. Bandoli, D. Barreca, A. Gasparotto, C. Maccato, R. Seraglia, E. Tondello, A. Devi, R. A. Fischer, M. Winter, *Inorg. Chem.* **2009**, *48*, 82–89; b) G. Bandoli, D. Barreca, A. Gasparotto, R. Seraglia, E. Tondello, A. Devi, R. A. Fischer, M. Winter, E. Fois, A. Gambae, G. Tabacchi, *Phys. Chem. Chem. Phys.* **2009**, *11*, 5998–6007; c) D. Barreca, G. Carraro, A. Devi, E. Fois, A. Gasparotto, R. Seraglia, C. Maccato, C. Sada, G. Tabacchi, E. Tondello, A. Venzo, M. Winter, *Dalton Trans.* **2012**, *41*, 149–155; d) A. Gasparotto, D. Barreca, A. Devi, R. A. Fischer, E. Fois, A. Gamba, C. Maccato, R. Seraglia, G. Tabacchi, E. Tondello, *ECS Trans.* **2009**, *25*, 549–556; e) P.-S. J. J. P. Fackler, *Inorg. Chem.* **1973**, *12*, 1174–1182; f) G. Malandrino, M. Blandino, L. M. S. Perdicaro, I. L. Fragala, P. Rossi, P. Dapporto, *Inorg. Chem.* **2005**, *44*, 9684–9689; g) G. Malandrino, S. T. Finocchiaro, P. Rossi, P. Dapporto, I. L. Fragala, *Chem. Commun.* **2005**, 5681–5683; h) J. Ni, H. Yan, A. Wang, Y. Yang, C. L. Stern, A. W. Metz, S. Jin, L. Wang, T. J. Marks, J. R. Ireland, C. R. Kannewurf, *J. Am. Chem. Soc.* **2005**, *127*, 5613–5624.

[26] a) C. C. Roberts, B. R. Barnett, D. B. Green, J. M. Fritsch, *Organometallics* **2012**, *31*, 4133–4141; b) C. Di Iulio, M. Middleton, G. Kociok-Köhn, M. D. Jones, A. L. Johnson, *Eur. J. Inorg. Chem.* **2013**, 1541–1554; c) K. A. Gerling, N. M. Rezayee, A. L. Rheingold, D. B. Green, J. M. Fritsch, *Dalton Trans.* **2014**, *43*, 16498–16508; d) C. Scheiper, D. Dittrich, C. Wölper, D. Bläser, J. Roll, S. Schulz, *Eur. J. Inorg. Chem.* **2014**, 2230–2240.

[27] a) J. Holmes, K. Johnson, B. Zhang, H. E. Katz, J. S. Matthews, *Appl. Organomet. Chem.* **2012**, *26*, 267–272; b) D. Bekermann, A. Ludwig, T. Toader, C. Maccato, D. Barreca, A. Gasparotto, C. Bock, A. D. Wieck, U. Kunze, E. Tondello, R. A. Fischer, A. Devi, *Chem. Vapor Depos.* **2011**, *17*, 155–161.

[28] J. A. Manzi, C. E. Knapp, I. P. Parkin, C. J. Carmalt, *Eur. J. Inorg. Chem.* DOI:10.1002/ejic.201500416.

[29] D. L. Schulz, B. J. Hinds, D. A. Neumayer, C. L. Stern, T. J. Marks, *Chem. Mater.* **1993**, *5*, 1605–1617.

[30] a) A. M. Willcocks, T. Pugh, S. D. Cosham, J. Hamilton, S. L. Sung, T. Heil, P. R. Chalker, P. A. Williams, G. Kociok-Köhn, A. L. Johnson, *Inorg. Chem.* **2015**, *54*, 4869–4881; b) S. A. Rushworth, L. M. Smith, A. J. Kingsley, R. Odedra, R. Nickson, P. Hughes, *Microelectron. Reliab.* **2005**, *45*, 1000–1002.

[31] N. Matsubara, T. Kuwamoto, *Inorg. Chem.* **1985**, *24*, 2697–2701.

[32] C. S. McNally, D. P. Turner, A. N. Kulak, F. C. Meldrum, G. Hyett, *Chem. Commun.* **2012**, *48*, 1490–1492.

[33] M. Caglar, Y. Caglar, S. Ilican, *J. Optoelectron. Adv. Mater.* **2006**, *8*, 1410–1413.

[34] L. J. Farrugia, *J. Appl. Crystallogr.* **1999**, *32*, 837–838.

[35] T. Maruyama, S. Arai, *Sol. Energy Mater. Sol. Cells* **1993**, *30*, 257–262.

Received: May 19, 2015
Published Online: August 24, 2015

